Dalton Transactions
An international journal of inorganic chemistry

This article can be cited before page numbers have been issued, to do this please use: Y. Liu, J. Ma, P. Wu, J. Zheng, X. Tian, M. Jiang, Y. He, H. Dong and J. Wang, *Dalton Trans.*, 2019, DOI: 10.1039/C9DT01763A.

ROYAL SOCIETY
OF CHEMISTRY

rsc.li/dalton

View Article Online
DOI: 10.1039/C9DT01763A

ARTICLE

Nanoporous Metal–organic Framework as Renewable Size-selective Hydrogen-Bonding Catalyst in Water

Received 00th January 20xx,
Accepted 00th January 20xx

DOI: 10.1039/x0xx00000x

Yanhong Liu,[a†] Ju Ma,[a†] Pengyan Wu,*[a] Jia-Jia Zheng,[b] Xueqin Tian,[a] Min Jiang,[a] Yumei He,[a] Han Dong[a] and Jian Wang*[a]

A novel squaramide-containing metal–organic framework (MOF) material has been designed and synthesized. Detailed X-ray crystal structure analysis showed that four squaramides of this MOF adopted two orientations in each dependent nanopore, confirming that two carbonyl and two N-H groups pointed simultaneously to the inside of the one-dimensional nanometer channel. The MOF was applied as an efficient bifunctional hydrogen-bonding catalyst for Michael additions of 1,3-dicarbonyl compounds to nitroalkenes in pure water, boosting the catalytic efficiency by up to approximately five times the value afforded by the homogeneous control, as well as exhibiting a highly size-selective catalytic performance and good renewability. The catalytic mechanism was also discussed in detail. The present study provides a highly promising approach to achieving dual-activation catalytic centers in a single system, which function as microscopic chemical reactors that allow interaction and fast transport of substrate molecules in their cavities.

Introduction

Inspired by their natural ability, synthetic chemists have long sought to mimic the properties of biological systems using abiotic platforms.[1] This is due to their potential for developing synthetically useful catalysts that match or even exceed the capabilities of natural systems.[2] Considering the pivotal role of H-bonding in myriad natural processes, hydrogen-bond (HB) organocatalysis has emerged as a biomimetic alternative to enzyme catalysis, which can activate electrophilic moieties toward nucleophilic addition *via* cooperative hydrogen bonding.[3,4] Metal–organic frameworks (MOFs) or porous coordination polymers (PCPs) are crystalline materials with extended structures that can be utilized in many fields, such as gas sorption,[5,6] sensing and optical,[7,8] drug delivery,[9] and catalysis.[10–12] In recent years, MOFs were studied as novel heterogeneous catalysts because of their tunability, permanent microporosity, and defined reaction environments.[13] Moreover, the extensive distribution of active sites and confined inner spaces in MOFs make them excellent enzyme-like catalysts possessing the integrated advantages of heterogeneous and homogeneous catalysis, such as size-selectivity, easy separation and recycling, and high activity.[14,15] Despite these advances, the rational design of efficient enzyme-like MOF catalysts remains difficult.

Squaramide derivatives are powerful hydrogen-bonding organocatalysts for key bond-forming transformations among many eligible HB catalysts reported to mimic biological machinery.[16,17] This is not only owing to squaramides derived from squaric acid possessing hydrogen-bond accepting and donating functionalities through their carbonyl and N–H groups, respectively, but also because of their improved acidity originating from the potential for resonance stabilization of enhanced electron density of the partially aromatic squaramide ring.[18] However, their strong hydrogen-bonding ability also drives self-aggregation and salvation to form dimers or oligomers, causing deactivation during the homogeneous catalysis[19] and resulting in serious recycling issues.

Based on the above MOF characteristics, incorporating squaramide derivatives as pillaring struts into MOFs would prevent detrimental self-association due to their ordered structure. However, squaramide-containing MOFs are rare;[20] *e.g., Hupp, Farha,* and *Mirkin et al.* first demonstrated the functionalization of a heterogeneous framework with an acidic squaramide derivative for the biorelevant Friedel–Crafts reaction between β-nitrostyrene and indole; *Cohen et al.* used a new squaramide-based ligand to construct MOFs as active catalysts for the Friedel–Crafts reaction; our group has also constructed a novel squaramide-containing MOF for the luminescence-selective detection of lactose in aqueous solution and in milk. To the best of our knowledge, there are no reports of squaramide-containing MOFs as bifunctional hydrogen-bonding donor-acceptor catalysts for one reaction, because it is very difficult to control the distribution and configuration of squaramide moieties inside the pore cavities of the designed MOFs. Herein, we report the synthesis of a new squaramide-containing MOF, which is formed by using 3,3'-((3,4-dioxocyclobut-1-ene-1,2-diyl)bis(azanediyl))dibenzoic acid and $Zn(NO_3)_2·6H_2O$ under solvothermal conditions. We envisioned that the well-positioned

---

[a] School of Chemistry and Materials Science & Jiangsu Key Laboratory of Green Synthetic Chemistry for Functional Materials, Jiangsu Normal University, Xuzhou, 221116, P. R. China. E-mail: wpyan@jsnu.edu.cn; wjian@jsnu.edu.cn
[b] Institute for Integrated Cell-Material Sciences (WPI-iCeMS), Kyoto University, Ushinomiya cho, Yoshida, Sakyo-ku, Nishikyo-ku, Kyoto 606-8501, Japan.

† These authors contributed equally to this work.

Electronic Supplementary Information (ESI) available: Additional experimental details, crystal data and related spectra. See DOI: 10.1039/x0xx00000x

DOI: 10.1039/C9DT01563A

squaramide group orientation and the catalytic sites within the large pores of this MOF would combine HB accepting and donating bifunctionality to activate the catalytic substrates. This MOF shows good catalytic activity toward Michael addition of nitroalkenes and 1,3-dicarbonyl compounds in the heterogeneous state and displays size-selective catalytic behavior for a large substrate scope in water.

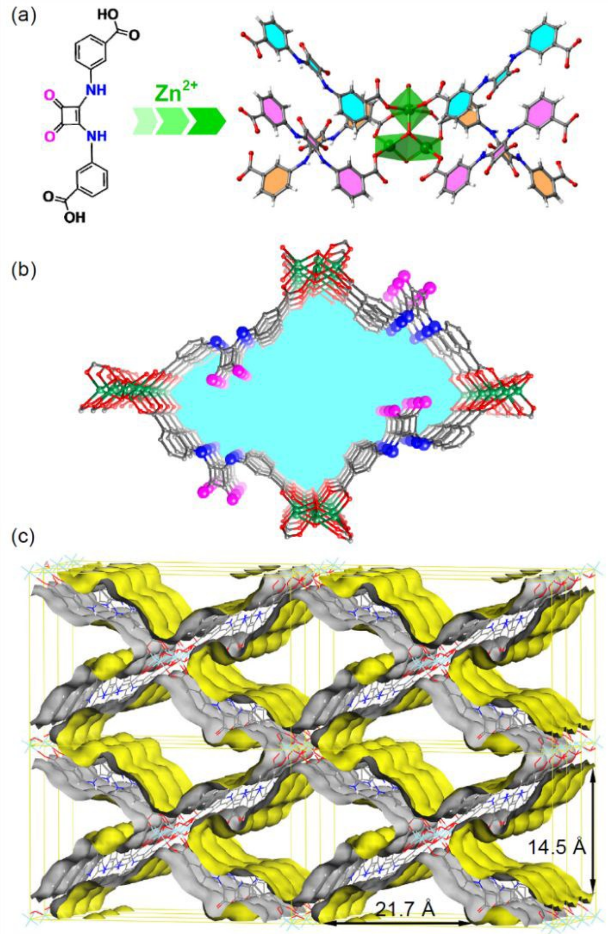

Figure 1. (a) Construction of Zn–DBDA consolidated by squaramide-based ligands and coordinated environment of Zn^{2+} ions in Zn–DBDA. (b) Two N–H moieties and two carbonyl moieties from four different squaramide-based ligands as potential catalytically active sites pointing to the inside of the nanometer 1D channel. (c) Connolly surface (radius: 1.4 Å) of Zn–DBDA along the [100] direction. Gray represents the outer surfaces of the channels, while yellow represents their inner surfaces. For clarity, the hydrogen atoms are omitted in (b).

Results and discussion

Crystallographic description of Zn–DBDA

The solvothermal reaction of $Zn(NO_3)_2 \cdot 6H_2O$ and 3,3'-((3,4-dioxocyclobut-1-ene-1,2-diyl)bis(azanediyl))dibenzoic acid (H_2dbda) in N,N-dimethylformamide (DMF)/ethanol gave the pale-yellow block crystal Zn–DBDA $\{Zn_{1.5}(OH)(dbda)\cdot 5DMF\}_n$ in high yield (85%). Zn–DBDA was determined by single-crystal X-ray diffraction to crystallize in the monoclinic space group *P*2(1)/*c* and was found to be a three-dimensional framework containing infinite one-dimensional $[Zn_3O_8(OH)_2]_n$ chains connected through the $dbda^{2-}$ ligands. In an asymmetric unit of the $[Zn_3O_8(OH)_2]_n$ chains, two zinc atoms adopt tetrahedral coordination geometry with two oxygen atoms of two different carboxylate ligands and two others belonging to hydroxyl groups; the other crystallographic zinc atom is octahedrally coordinated to four oxygen atoms belonging to the carboxylate groups of four $dbda^{2-}$ ligands and two oxygen atoms belonging to hydroxyl groups (Figure 1a and Figure S1 in the SI).

The Zn–O bond distances are 1.91(0)–2.12(7) Å. The infinite zinc oxyhydroxide chain can be regarded as a secondary building unit (SBU). These chains, which are parallel to the *a*-axis, are further interconnected through the $dbda^{2-}$ moieties to generate a three-dimensional architecture. It is noteworthy that the $dbda^{2-}$ ligands in Zn–DBDA all showed a μ_4-η^1:η^1:η^1:η^1 coordination mode (Figure S2 in the SI). A one-dimensional nanometer channel with a cross-section of 21.7 × 14.5 $Å^2$ (based on the van der Waals radii of the atoms) was viewed along the [100] direction (Figure 1c). In each dependent channel, two N–H and two carbonyl moieties from four different squaramide-based ligands point to the inside of the pore cavity (Figure 1b), facilitating interaction and activation of the hydroxyl or related moieties in the substrates. The solvent-accessible volume was calculated as 1,865.8 $Å^3$ using the PLATON program, which is 55.0% of the unit-cell volume. The Brunauer–Emmett–Teller surface area calculated from CO_2 sorption data for Zn–DBDA was 342 m^2 g^{-1} (Figure S3 in the SI). The thermogravimetric analysis (TGA) curve of Zn–DBDA showed that its structure could be maintained up to 430°C, with a weight loss of 43.7% between 26°C and 430°C corresponding to the loss of five DMF molecules (calculated as 44.04%) (Figure S4 in the SI); additionally, TGA clearly indicated that the guest molecules were completely excluded after Zn–DBDA was dried at 120°C under vacuum. Interestingly, the index of powder XRD patterns of the Zn–DBDA bulk sample immersed in water for 7 days evidenced maintenance of the framework, indicating the feasibility of Zn–DBDA as a sensing or catalytic material in aqueous solution (Figure S5 in the SI).

Table 1. Optimization and control experiments of Michael addition of Hacac with β-nitrostyrene.[a)]

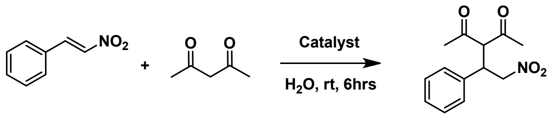

Entry	Catalyst	Solvent	Yields[b)]
1	$Zn(NO_3)_2$	H_2O	n.d.
2	H_2dbda	H_2O	19
3	$Zn(NO_3)_2/H_2dbda$	H_2O	20
4	---	H_2O	n.d.
5	Zn–DBDA	H_2O	>99

[a)] Reaction conditions: Zn–DBDA (5.0 μmol of squaramide based on TGA), β-nitrostyrene (0.1 mmol), Hacac (0.2 mmol), 3.0 mL of water, reaction time: 6 h; [b)] Determined by ^1H NMR.

Catalytic experiments on Michael addition

Our catalytic experiments were focused on Michael addition of nitroolefins and dicarbonyl compounds.[21] The catalytic activity of activated Zn–DBDA as a catalyst was assessed for Michael addition of acetylacetone (Hacac) with β-nitrostyrene as a model reaction, where the reaction was conducted in a flask with 0.1 mmol of β-

View Article Online
DOI: 10.1039/C9DT01763A

nitrostyrene, 0.2 mmol of Hacac, and 0.5 mol% of Zn–DBDA as a catalyst in 3 mL of H_2O at room temperature, giving a yield of >99%, which shows that Zn–DBDA is an effective catalyst for Michael addition of β-nitrostyrene and Hacac. Simultaneously, a series of controlled experiments were investigated under the same conditions to eliminate the factors affecting catalytic performance and unveil the catalytic nature of Zn–DBDA. A reaction conducted in the absence of Zn–DBDA yielded no detectable conversion. The use of the ligand H_2dbda itself rather than Zn–DBDA as the catalyst gave a yield of only 19% (Table 1, entries 4 and 2), while $Zn(NO_3)_2$ displayed no catalytic activity under the same conditions; even a simple mixture of $Zn(NO_3)_2$ and H_2dbda afforded only similar conversion to that of the ligand itself (Table 1, entries 1 and 3). These results revealed that this squaramide-containing MOF Zn–DBDA can serve as an excellent catalyst for the Michael addition reaction, facilitating close proximity between squaramide groups governing catalytic functional groups and the substrates within confined spaces.

Table 2. Evaluation of Zn–DBDA in catalytic Michael addition reactions of various β-nitroolefins with Hacac.[a)]

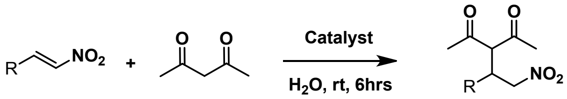

Entry	β-nitrostyrenes	Molecular Size	Yields[b)]
1	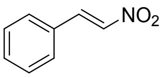	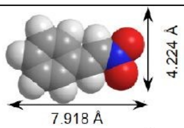	>99
2	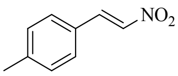	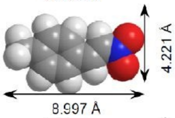	95
3	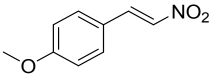	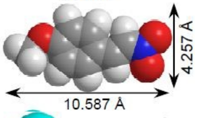	91
4	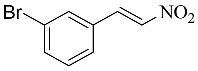	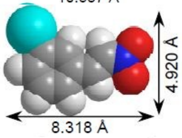	93
5	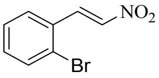	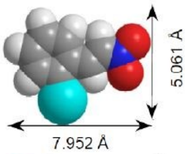	91
6	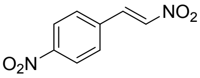	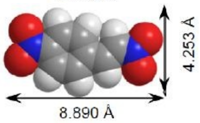	86
7	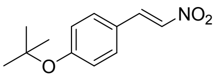	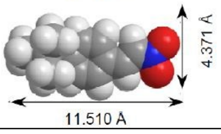	25

[a)] Reaction conditions: Zn–DBDA (5.0 μmol of squaramide based on TGA), β-nitroolefins (0.1 mmol), Hacac (0.2 mmol), 3.0 mL of water, reaction time: 6 h; [b)] Determined by ^1H NMR.

With these optimal reaction conditions in hand, we further surveyed the generality and scope of the present protocol across a range of β-nitroolefins with Hacac in the presence of 0.5 mol% of Zn–DBDA. As summarized in Table 2, the reactions of all β-nitroolefins having electron-donating substituents such as methyl and methoxy or electron-withdrawing substituents such as bromine at the *ortho*- and *meta*-positions, and nitro, with Hacac gave the corresponding Michael adducts in high yield (reaching 85%). When the reactant was the bulky nitrostyrene, (E)-1-(tert-butoxy)-4-(2-nitrovinyl)benzene, the reaction gave a dramatically decreased yield, with only 25% product conversion (Table 2, Entry 7). It is speculated that the large β-nitroolefins have limited access to catalytic sites inside the MOF tunnel, preventing easy attainment of suitable transition-state geometry, thus exerting size-selective catalysis.

Table 3. Evaluation of Zn–DBDA in catalytic Michael addition reactions of various 1,3-dicarbonyl compounds with β-nitrostyrene.[a)]

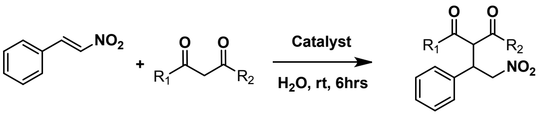

Entry	1,3-dicarbonyls	Molecular Size	Yields[b)]
1	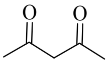	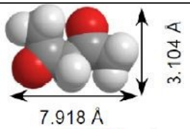	>99
2	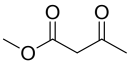	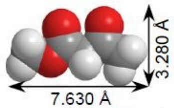	95
3	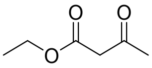	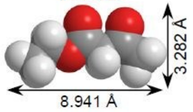	90
4	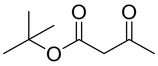	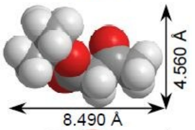	33
5	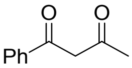	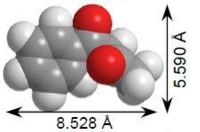	3
6	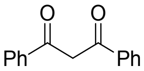	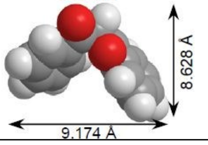	n.d.

[a)] Reaction conditions: Zn–DBDA (5.0 μmol of squaramide based on TGA), β-nitrostyrene (0.1 mmol), 1,3-dicarbonyl compounds (0.2 mmol), 3.0 mL of water, reaction time: 6 h; [b)] Determined by ^1H NMR.

Encouraged by these results, the substrate scope of the reaction was also investigated with several 1,3-dicarbonyl compounds as nucleophiles. As shown in Table 3, more than 90% of Michael products were detected when methyl 3-oxobutanoate and ethyl 3-oxobutanoate were used (Table 3, entries 2 and 3). Conversely, as the molecular sizes of the 1,3-dicarbonyl substrates increased, a

View Article Online
DOI: 10.1039/C9DT01763A

significant decrease in the yield of Michael products was observed, as shown by the 33% formation of *tert*-butyl 2-acetyl-4-nitro-3-phenylbutanoate (Table 3, entry 4). The presence of 1-phenylbutane-1,3-dione resulted in only a trace yield (about 3%) under the same experimental conditions (Table 3, entry 5). A bulkier substrate, 1,3-diphenylpropane-1,3-dione, was employed, resulting in inefficient Michael addition with an undetectable yield (Table 3, entry 6). This size-selective catalysis with comparable reactivity provides further evidence that the catalytic reactions might occur in the channels of Zn–DBDA and that the two substrates might be simultaneously activated in the same channel. All the results demonstrated that Zn–DBDA was an efficient size-selective catalyst toward Michael addition reactions.

Catalytic mechanism discussion

To further verify and understand the catalysis, a luminescence titration between Zn–DBDA and β-nitrostyrene or Hacac was further applied to investigate the interaction between the catalyst and substrates. Upon excitation at 320 nm, Zn–DBDA showed an intense luminescence band at about 470 nm, derived from ligand-based emission. Adding 0.23 mM β-nitrostyrene to 0.55 mM Zn–DBDA suspension led to approximately 71% quenching of the emission intensity of the Zn–DBDA, with a Stern–Volmer constant (K_{SV}) calculated as 9.24 ± 0.12 × 10^3 M^{-1} (Figure 2a and Figure S6 in the SI). It is noteworthy that fluorescence titration upon adding Hacac also revealed 65% quenching of the Zn–DBDA emission with a K_{SV} of 2.37 ± 0.1 × 10^3 M^{-1} (Figure S7 in the SI). The results indicated that both Hacac and β-nitrostyrene can interact with Zn–DBDA.

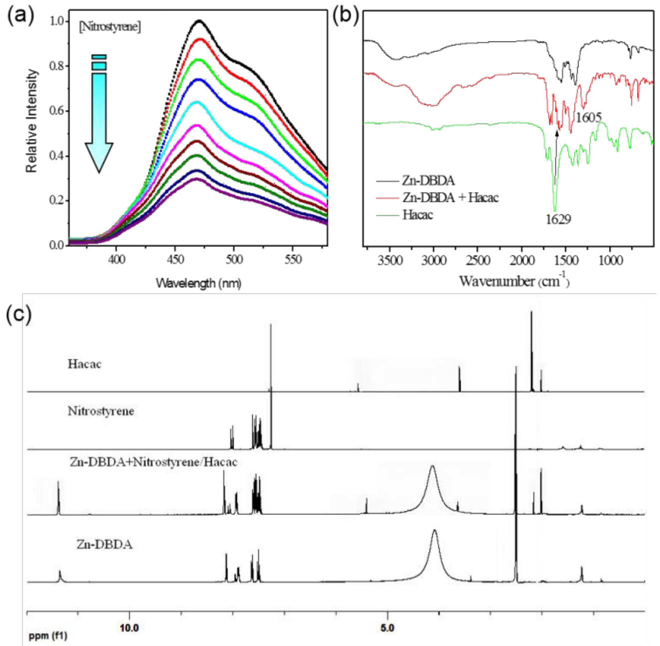

Figure 2. (a) Family of fluorescence spectra of Zn–DBDA (0.55 mM) upon adding β-nitrostyrene up to 0.23 mM. (b) FT-IR spectra of Zn–DBDA (top), Zn–DBDA obtained after absorption of Hacac (middle), and Hacac (bottom). (c) The ^{1}H-NMR spectra after nitrostyrene and Hacac adsorption in the Zn–DBDA.

Additionally, the desolvated Zn–DBDA was dispersed in a H_2O solution containing β-nitrostyrene or Hacac for one day. The filtered solid was then washed several times with water/ethanol to remove residual substrate from the surface. The IR spectrum of Zn–DBDA with absorbed β-nitrostyrene was compared to that of Zn–DBDA. A red shift occurred for the splitting of the peak at 1314 cm^{-1} belonging to the N=O stretching vibration, comparable with the corresponding peak in the spectrum of free β-nitrostyrene (1343 cm^{-1}) (Figure S8 in the SI). Additionally, the emerging peak at 1605 cm^{-1} for the Hacac-impregnated Zn–DBDA is attributed to the characteristic C=O stretching vibration peak and shows a red shift from 1629 cm^{-1} (for free Hacac) (Figure 2b and Figure S9 in the SI). This suggested that the adsorption of β-nitrostyrene and Hacac occurred within the MOF channels via weak interactions. Moreover, ^{1}H NMR analysis of the Zn–DBDA solid after immersion in a H_2O solution containing β-nitrostyrene and Hacac also demonstrated that Zn–DBDA could adsorb one molecular stoichiometric amount of β-nitrostyrene and Hacac per pore (Figure 2c and Figures S10 and S11 in the SI). Extensive molecular force field-based calculations were further performed to gain insight into the interaction between Zn–DBDA and β-nitrostyrene/Hacac by using a universal force field as implemented in the Gaussian 09 program. As shown in Scheme 1(A), close contacts were observed between the oxygen atoms of the carbonyl groups of squaramide moieties from Zn–DBDA and the hydrogen atoms from isomerized Hacac. Meanwhile, close contacts were also observed between the oxygen atoms of β-nitrostyrene and the N-H groups of squaramide moieties from Zn–DBDA, and the nearest O···H distances were only 2.38 and 2.16 Å, respectively, which are typical for hydrogen bonds; this result is also consistent with the experimental results. All the results indicated that both Hacac and β-nitrostyrene can be adsorbed in the channel of Zn–DBDA and further activated by the squaramide groups.

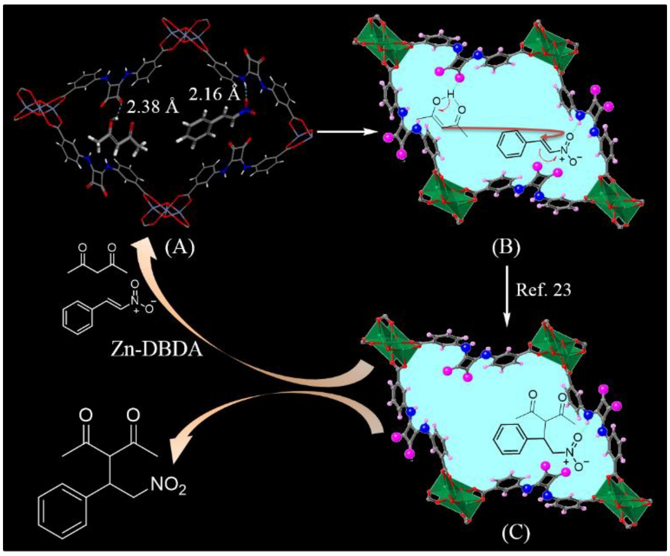

Scheme 1. Representation of the interaction between Zn–DBDA and β-nitrostyrene/Hacac computed by molecular force field-based calculations (A). Proposed mechanism of Michael addition catalyzed by Zn–DBDA (B and C).

Based on the above analysis and literature reports,[22] we propose a plausible dual-activation model for this Michael addition. As shown in Scheme 1, firstly, catalyst Zn–DBDA simultaneously activates nitroolefins and Hacac through hydrogen-bonding

View Article Online
DOI: 10.1039/C9DT01763A

interactions to form intermediate A. Then, nucleophilic attack (B) from the enolate to nitroolefins generates a new intermediate (C).[23] Finally, the nitronate takes the proton from the catalyst to provide the product along with regeneration of the Zn–DBDA catalyst.

Reproducibility

An essential feature of any catalyst from the viewpoint of industrial application is its reusability over multiple reaction cycles. We first demonstrated the heterogeneity of our catalytic system, and gravity filtration was performed to remove the catalyst after reacting for 2 h; the results demonstrated that the reaction was nearly terminated within the next 4 h (Figure S12 in the SI). Besides, at the end of the reaction, inductively coupled plasma (ICP) analysis of the reaction mixture filtrate revealed no Zn leaching, indicating that the catalytic reaction is indeed heterogeneous. Therefore, we investigated the catalytic activity and stability of Zn–DBDA samples isolated *via* filtration from the catalytic reaction. Prior to each catalytic run, Zn–DBDA was recovered and washed several times with water, then used again for catalytic Michael addition in a fresh solution. Hardly any loss of catalytic activity was observed; even when undergoing catalytic recycling five successive times, the yield of 3-(2-nitro-1-phenylethyl)pentane-2,4-dione remained nearly constant at 98% for the 2nd, 98% for the 3rd, 96% for the 4th, and 97% for the 5th run (Figure S13 in the SI). Furthermore, the powder X-ray diffraction patterns for the five cycles showed that the crystalline phase of Zn–DBDA remained unaltered, indicating that the catalyst structure was relatively stable during the reaction (Figure S5 in the SI). Such remarkably high recyclability, high efficiency, and size selectivity to substrates in catalytic Michael addition make this approach suitable not only for laboratory-scale research but also for industrial application.

Experimental

Synthesis of Zn–DBDA: A mixture of H_2dbda (8.8 mg, 5 mM) and $Zn(NO_3)_2 \cdot 6H_2O$ (30 mg, 20 mM) was dissolved in DMF/ethanol (4/1, 5 mL) in a screw-capped vial. The resulting mixture was placed in an oven at 80°C for 1 day. After cooling, pale-yellow block crystals were collected by filtration. Yield: 85%. Anal. calc. for $C_{24}H_{22}N_4O_9Zn_{1.5}$: C 47.37%, H 3.64%, N 9.2%; Found: C 47.21%, H 3.67%, N 9.32%.

General Procedure for Catalysis Experiments: The catalyst Zn–DBDA (0.01 mmol, based on Zn), nitroalkenes (1.0 mmol), Hacac (2.0 mmol), and 3.0 mL water were added sequentially to a 10 mL round-bottom flask. The mixture was allowed to react at 25°C for 6 h. During this time, the reaction was monitored constantly by TLC. After completion of the reaction, the heterogeneous catalyst was filtered through filter paper for the recycling experiment. The aqueous solution was extracted with Et_2O (3 × 3.0 mL). The combined Et_2O was washed twice with water and dehydrated with Na_2SO_4. After evaporation of Et_2O, the residue was purified by silica gel flash column chromatography to afford the desired product. The conversion was calculated from the ^1H NMR data.

Conclusions

In summary, a novel Zn(II)-based nanoporous MOF was synthesized by incorporating the squaramide moiety as the backbone, in which HB acceptor and donor sites existed simultaneously in each dependent pore cavity. The well-positioned squaramide group orientation and well-defined pores of the frameworks made this MOF an efficient bifunctional HB donor-acceptor catalyst for Michael addition of 1,3-dicarbonyl compounds to nitroolefins in water with good size-selectivity. The MOF was recycled by simple filtration and reused several times without significant loss of activity. This study provides a highly promising approach to achieving size-selective conversion by constructing dual-activation catalytic centers in a single system, which function as microscopic chemical reactors that allow interaction and fast transport of substrate molecules in their cavities.

Conflicts of interest

There are no conflicts to declare.

Acknowledgments

We gratefully acknowledge financial support from the Natural Science Foundation of Jiangsu Province for Outstanding Youth (No. BK20180105), the National Natural Science Foundation of China (Nos. 21401087 and 21401086), Postgraduate Research & Practice Innovation Program of Jiangsu Province (No. KYCX18_2103), PAPD and TAPP of Jiangsu Higher Education Institutions.

Notes and references

‡ Crystal data of Zn−DBDA: $C_{33}H_{45}N_7O_{12}Zn_{1.5}$, Mr = 829.8, Monoclinic, space group *P*2(1)/*c*, a = 5.9994(12), b = 29.661(6), c = 19.068(4) Å, α = 90.00, β = 90.09, γ = 90.00, V = 3393.0(12) $Å^3$, Z = 4, *D*c = 1.624 g cm^{-3}, μ(Mo-Kα) = 1.146 mm^{-1}, *T* = 296(2) K. 19212 unique reflections [R_{int} = 0.1398]. Final R_1[with $I > 2\sigma(I)$] = 0.0637, wR_2(all data) = 0.1262, GOOF = 1.003. CCDC number: 1810642.

1 D. J. Cram, *Angew. Chem., Int. Ed.*, 1988, **27**, 1009; J.-M. Lehn, *Angew. Chem., Int. Ed.*, 1988, **27**, 89; B. H. Northrop, Y. R. Zheng, K. W. Chi and P. J. Stang, *Acc. Chem. Res.*, 2009, **42**, 1554; M. Yoshizawa, M. Tamura and M. Fujita, *Science*, 2006, **312**, 251.

2 Y. Inokuma, M. Kawano and M. Fujita, *Nature Chem.*, 2011, **3**, 349; M. S. Rosen, C. L. Stern and C. A. Mirkin, *Chem. Sci.*, 2013, **4**, 4193.

3 P. R. Schreiner, *Chem. Soc. Rev.*, 2003, **32**, 289; H. Xu, S. J. Zuend, M. P. Woll, Y. Tao and E. N. Jacobsen, *Science*, 2010, **327**, 986.

4 X. Fang and C.-J. Wang, *Chem. Commun.*, 2015, **51**, 1185; E. T. Hennessy and E. N. Jacobsen, *Nature Chem.*, 2016, **8**, 741; V. J. Lillo, J. Mansilla and J. M. Saá, *Angew. Chem., Int. Ed.*, 2016, **55**, 4312; P. R. Schreiner and A. Wittkopp, *Org. Lett.*, 2002, **4**, 217.

5 R. W. Flaig, T. M. Osborn Popp, A. M. Fracaroli, E. A. Kapustin, M. J. Kalmutzki, R. M. Altamimi, F. Fathieh, J. A. Reimer and O. M. Yaghi, *J. Am. Chem. Soc.*, 2017, **139**, 12125; J.-R. Li, R. J. Kuppler and H.-C. Zhou, *Chem. Soc. Rev.*, 2009,

38, 1477; O. K. Farha, A. O. Yazaydin, I. Eryazici, C. D. Malliakas, B. G. Hauser, M. G. Kanatzidis, S. T. Nguyen, R. Q. Snurr and J. T. Hupp, *Nature Chem.*, 2010, **2**, 944.

6 L. J. Murray, M. Dinča and J. R. Long, *Chem. Soc. Rev.*, 2009, **38**, 1294; J. G. Duan, M. Higuchi, M. L. Foo, S. Horike, K. P. Rao and S. Kitagawa, *Inorg. Chem.*, 2013, **52**, 8244; X.-P. Wang, W.-M. Chen, H. Qi, X.-Y. Li, C. Rajnák, Z.-Y. Feng, M. Kurmoo, R. Boča, C.-J. Jia, C.-H. Tung and D. Sun, *Chem. Eur. J.*, 2017, **23**, 7990; Y.-Q. Lan, H.-L. Jiang, S.-L. Li and Q. Xu, *Adv. Mater.*, 2011, **23**, 5015.

7 B. L. Chen, S. Xiang and G. D. Qian, *Acc. Chem. Res.*, 2010, **43**, 1115; W. P. Lustig, S. Mukherjee, N. D. Rudd, A. V. Desai, J. Li and S. K. Ghosh, *Chem. Soc. Rev.*, 2017, **46**, 3242; Y. Zhao, X. Y. Xu, L. Qiu, X. J. Kang, L. L. Wen and B. G. Zhang, *ACS Appl. Mater. Interfaces*, 2017, **9**, 15164; S. Wang, T. Cao, H. Yan, Y. Li, J. Lu, R. Ma, D. Li, J. Dou and J. Bai, *Inorg. Chem.*, 2016, **55**, 5139; S.-S. Zhang, X. Wang, H.-F. Su, L. Feng, Z. Wang, W.-Q. Ding, V. A. Blatov, M. Kurmoo, C.-H. Tung, D. Sun and L.-S. Zheng, *Inorg. Chem.*, 2017, **56**, 11891;

8 Y. Wang, G. Ye, H. Chen, X. Hu, Z. Niu and S. Ma, *J. Mater. Chem. A*, 2015, **3**, 15292; Z. Wang, X.-Y. Li, L.-W. Liu, S.-Q. Yu, Z.-Y. Feng, C.-H. Tung and D. Sun, *Chem. Eur. J.*, 2016, **22**, 6830; M.-L. Han, G.-X. Wen, W.-W. Dong, Z.-H. Zhou, Y.-P. Wu, J. Zhao, D.-S. Li, L.-F. Ma and X. Bu, *J. Mater. Chem. C*, 2017, **5**, 8469; T.-Q. Song, K. Yuan, W.-Z. Qiao, Y. Shi, J. Dong, H.-L. Gao, X.-P. Yang, J.-Z. Cui and B. Zhao, *Anal. Chem.*, 2019, **91**, 2595; X. Mi, D. Sheng, Y. Yu, Y. Wang, L. Zhao, J. Lu, Y. Li, D. Li, J. Dou, J. Duan and S. Wang, *ACS Appl. Mater. Interfaces*, 2019, **118**, 7914.

9 P. Horcajada, T. Chalati, C. Serre, B. Gillet, C. Sebrie, T. Baati, J. F. Eubank, D. Heurtaux, P. Clayette, C. Kreuz, J. S. Chang, Y. K. Hwang, V. Marsaud, P. N. Bories, L. Cynober, S. Gil, G. Ferey, P. Couvreur and R. Gref, *Nature Mater.*, 2010, **9**, 172; J. D. Rocca, D. M. Liu and W. B. Lin, *Acc. Chem. Res.*, 2011, **44**, 957; J. S. Qin, D. Y. Du, W. L. Li, J. P. Zhang, S. L. Li, Z. M. Su, X. L. Wang, Q. Xu, K. Z. Shao and Y. Q. Lan, *Chem. Sci.*, 2012, **3**, 2114.

10 M. Yoon, R. Srirambalaji and K. Kim, *Chem. Rev.*, 2012, **112**, 1196; J. Y. Lee, O. K. Farha, J. Roberts, K. A. Scheidt, S. T. Nguyen and J. T. Hupp, *Chem. Soc. Rev.*, 2009, **38**, 1450; K. Manna, P. Ji, Z. Lin, F. X. Greene, A. Urban, N. C. Thacker and W. B. Lin, *Nature Commun.*, 2016, **7**, 12610.

11 L. Wang, D. W. Agnew, X. Yu, J. S. Figueroa and S. M. Cohen, *Angew. Chem. Int. Ed.*, 2018, **57**, 511; Z. Ju, S. Yan and D. Yuan, *Chem. Mater.*, 2016, **28**, 2000; P. Y. Wu, C. He, J. Wang, X. J. Peng, X. Z. Li, Y. L. An and C. Y. Duan, *J. Am. Chem. Soc.*, 2012, **134**, 14991; G.-W. Xu, Y.-P. Wu, W.-W. Dong, J. Zhao, X.-Q. Wu, D.-S. Li and Q. Zhang, *Small*, 2017, **13**, 1602996.

12 S. Yuan, J.-S. Qin, H.-Q. Xu, J. Su, D. Rossi, Y. Chen, L. Zhang, C. Lollar, Q. Wang, H.-L. Jiang, D. H. Son, H. Xu, Z. Huang, X. Zou and H.-C. Zhou, *ACS. Cent. Sci.*, 2018, **4**, 105; W. Zhou, D.-D. Huang, Y.-P. Wu, J. Zhao, T. Wu, J. Zhang, D.-S. Li, C. Sun, P. Feng and X. Bu, *Angew. Chem. Int. Ed.*, 2019, **58**, 4227; J.-D. Xiao and H.-L. Jiang, *Acc. Chem. Res.*, 2019, **52**, 356; Y. W. Peng, Z. G. Hu, Y. J. Gao, D. Q. Yuan, Z. X. Kang, Y. H. Qian, N. Yan and D. Zhao, *ChemSusChem*, 2015, **8**, 3208.

13 Y. B. Huang, J. Liang, X. S. Wang and R. Cao, *Chem. Soc. Rev.*, 2017, **46**, 126; M. Rimoldi, A. J. Howarth, M. R. DeStefano, L. Lin, S. Goswami, P. Li, J. T. Hupp and O. K. Farha, *ACS Catal.*, 2017, **7**, 997.

14 M. Zhao, S. Ou and C.-D. Wu, *Acc. Chem. Res.*, 2014, **47**, 1199; Z.-Y. Gu, J. Park, A. Raiff, Z. Wei and H.-C. Zhou, *ChemCatChem*, 2014, **6**, 67.

15 W.-Y. Gao, M. Chrzanowski and S. Ma, *Chem. Soc. Rev.*, 2014, **43**, 5841; P. Z. Li, X. J. Wang, J. Liu, J. S. Lim, R. Q. Zou and Y. L. Zhao, *J. Am. Chem. Soc.*, 2016, **138**, 2142.

16 R. I. Storer, C. Aciro and L. H. Jones, *Chem. Soc. Rev.*, 2011, **40**, 2330; J. P. Malerich, K. Hagihara and V. H. Rawal, *J. Am. Chem. Soc.*, 2008, **130**, 14416.

17 Y. Wang, J. Pan, R. Jiang, Y. Wang and Z. Zhou, *Adv. Synth. Catal.*, 2016, **358**, 195; H. Zhang, S. Lin and E. N. Jacobsen, *J. Am. Chem. Soc.*, 2014, **136**, 16485.

18 P. Chauhan, S. Mahajan, U. Kaya, D. Hack and D. Enders, *Adv. Synth. Catal.*, 2015, **357**, 253; J. Alemán, A. Parra, H. Jiang and K. A. Jørgensen, *Chem. Eur. J.*, 2011, **17**, 6890.

19 C. E. Silva, H. F. Dos Santos, N. L. Speziali, R. Diniz and L. F. C. de Oliveira, *J. Phys. Chem. A*, 2010, **114**, 10097; N. Busschaert, I. L. Kirby, S. Young, S. J. Coles, P. N. Horton, M. E. Light and P. A. Gale, *Angew. Chem., Int. Ed.*, 2012, **51**, 4426.

20 C. M. McGuirk, M. J. Katz, C. L. Stern, A. A. Sarjeant, J. T. Hupp, O. K. Farha and C. A. Mirkin, *J. Am. Chem. Soc.*, 2015, **137**, 919; X. P. Zhang, Z. J. Zhang, J. Boissonnault and S. M. Cohen, *Chem. Commun.*, 2016, **52**, 8585; M. Jiang, P. Li, P. Wu, F. Zhang, X. Tian, C. Deng and J. Wang, *Chem. Commun.*, 2018, **54**, 9131.

21 S. Lancianesi, A. Palmieri and M. Petrini, *Chem. Rev.*, 2014, **114**, 7108; J. P. Malerich, K. Hagihara and V. H. Rawal, *J. Am. Chem. Soc.*, 2008, **130**, 14416.

22 M. Bera, T. K. Ghosh, B. Akhuli and P. Ghosh, *J. Mol. Catal. A-Chem.*, 2015, **408**, 287; S. J. Connon, *Chem. Eur. J.*, 2006, **12**, 5418.

23 C. Min, X. Han, Z. Liao, X. Wu, H.-B. Zhou and C. Dong, *Adv. Synth. Catal.*, 2011, **353**, 2715; B. Kotai, G. Kardos, A. Hamza, V. Farkas, I. Papai and T. Soos, *Chem. Eur. J.*, 2014, **20**, 5631; Z. Dong, G. Qiu, H.-B. Zhou and C. Dong, Tetrahedron-Asymmetr., 2012, **23**, 1550.